

Chapter 3

Molecular Dynamics Simulation of Mouse MrgC11 Receptor with Bound F-(D)M-R-F-NH₂ in Explicit Lipid/Water Environment

3.1 Introduction

GPCR belongs to one of the membrane protein families embedded into the lipid bilayers, while the intra- and extracellular regions are exposed to the aqueous media. The membrane environment influences the function of membrane proteins, through electrostatic and steric interaction as well as through the membrane's internal pressure. Therefore the proper environment should be taken into account in the molecular simulation. However the resulting calculation, incorporating proteins, lipid bilayers, water molecules and ions needs to handle with 50,000 atoms even for the small proteins and this large simulation size poses a major computational challenge. Thanks to advances in computing power and availability of an efficient parallel molecular dynamics (MD) code, computational biologists have succeeded in performing the required calculations. Recently an all-atom molecular dynamics simulation of a complete virus system composed of 1 million atoms was presented by the Schulten group in the University of Illinois at Urbana-Champaign, using a parallel molecular dynamics program NAMD[1].

In chapter 2, in order to reduce the computation cost, the minimally required molecular components were considered in predicting the protein structure and the binding site. However our predicted mMrgC11 receptor structure was sufficiently accurate to identify binding sites for selective ligands, i.e. chirally modified tetrapeptides of F-M-R-F-NH₂. Therefore our structure prediction and docking methods might be good enough to predict the interaction between ligand

and GPCR. Nevertheless, it is worth performing MD studies for the mMrgC11/ligand complex structure in more realistic environments. These could provide the validation for our predicted structure and also information about the dynamic behavior, which might lead to understanding the role of conformational change on receptor activation.

Here we have carried out the all-atom MD simulation for mMrgC11/F-(D)M-R-F-NH₂ complex structure in explicit lipid and water environments, using NAMD 2.5 program[2]. In the following sections the detailed simulation procedure and the structural characteristics observed in a 7ns simulation run are described, focusing on the behavior of the ligand in the binding pocket and the conformational change on the transmembrane (TM) domains.

3.2 Simulation procedure

3.2.1 Setup of lipid and water environment

A molecular graphics program, Visual Molecular Dynamics (VMD) was used for the simulation setup. The Biograf file of the final optimized mMrgC11/F-(D)M-R-F-NH₂ complex structure was split into separate ligand and the receptor files. The hydrogen atoms were removed and the structure files were converted into PDB format compatible in VMD. The hydrogen atoms were then re-assigned with the estimated coordinates based on entries of internal coordinates present in the CHARMM topology dictionary. The N-terminus was acetylated (residue name: ACP in the CHARMM topology dictionary) and the C-terminus was capped with the N-methylamide group (residue name: CT3). The PDB and PSF files for the receptor and the ligand were then combined, generating a single PDB and PSF file respectively.

The complex structure was replaced for the mid-plan perpendicular to the TM helical axis to be positioned at $z = 0$. The equation of the mid-plane ($Ax+By+Cz+D = 0$) was calculated for the receptor using MembComp program[3]. Briefly, the hydrophobic center which showed the maximum hydrophobicity on the hydrophobicity profile was previously determined for each TM

helix. The plane of intersection was aligned to these seven points utilizing a least square approach. The origin of the plane was the geometric center of the centers defined for each helix. With this equation, the coordinates of the complex structure were transformed. Here the plane was moved to $z = 0$ and the vector normal to the plane became the z -axis. Also the origin of the plane was set to the geometric center of TM α -helices.

Next, the complex structure was then superimposed on the 75 Å x 75 Å slab of a solvated palmitoyl-oleoyl-phosphatidylcholine (POPC) lipid bilayer patch and the lipids and water molecules overlapping with the protein were removed (POPC within 1 Å and waters within 5 Å of the protein). The system was fully solvated with water by adding a ~30 Å thick slab from an equilibrated water box. The VMD autoionize plugin was then used to randomly place the ions necessary to neutralize the system. The resulting system was composed of 47,651 atoms; 4,180 receptor atoms, 74 ligand atoms, 4,288 lipid atoms, 39,087 water atoms and 10 chlorine atoms.

3.2.2 Molecular dynamics simulations

All simulations were performed with the parallel molecular dynamics code NAMD 2.5[2] using the CHARMM22 force field[4, 5] for proteins, the CHARMM27 parameters for the lipids and the TIP3P water model[6]. The simulated system was kept at constant temperature of 310 K by using Langevin dynamics for all non-hydrogen atoms, with a Langevin damping coefficient of 1 ps^{-1} . A constant pressure of 1 atm was maintained by using the Langevin piston method with a period of 200 fs and decay timescale of 200 fs.

Simulation was carried out with an integration time step of 1 fs. The bonded interaction was computed every time step; short-range nonbonded interaction every two time steps; and long-range electrostatic interaction every four time steps. A cutoff of 12 Å was used for van der Waals and short-range electrostatic interactions and a switching function started at 10 Å for van der Waals interactions to ensure a smooth cutoff. The simulation was performed under periodic

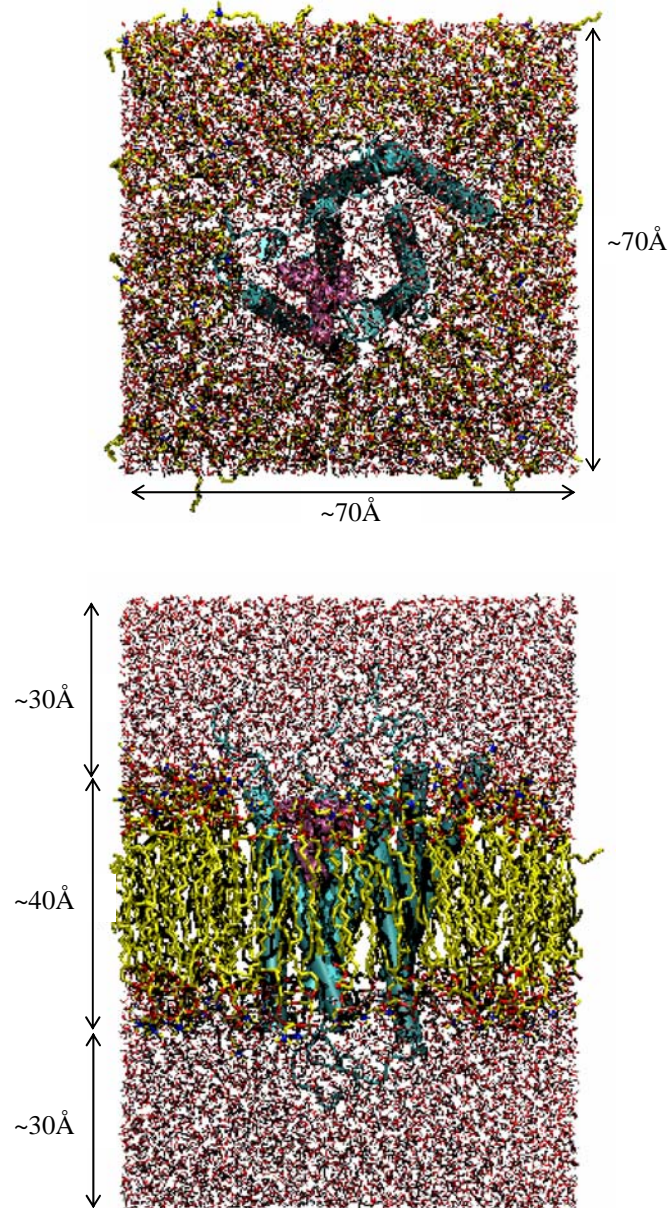


Figure 3.1 Fully solvated mMrgC11/F-(D)M-R-F-NH₂ complex in the membrane. It shows the final system built for NAMD run. The receptor (cyan) is shown in cartoon representation, the ligand (mauve) in VDW, lipids (yellow for carbon) in licorice and waters in line.

boundary condition with full electrostatics employed by using the Particle Mesh Ewald (PME) method.

Prior to full dynamics, the system was subjected to 5,000 steps of conjugate gradient energy minimization, followed by 100 ps of equilibration, while the coordinates of the receptor/ligand complex were fixed. In the equilibration, the system was gradually heated up from 0 K to 310 K by using Langevin dynamics with a damping coefficient of 5 ps^{-1} and the target temperature reached after ~ 7 ps. The system was again subjected to 5,000 steps of conjugate gradient energy minimization without any restraint. In energy minimization, the nonbonded interaction and electrostatic interaction were computed every time step. Lastly, the full dynamics simulation was carried out as described above.

The simulation was performed on a Linux-based cluster of Dual Intel Xenon 2.4 (or 3.06) GHz processors with 1 GB of memory per CPU. The first and second minimization took about 3 and 4 hours respectively with a single 3.06 GHz processor and the equilibration about 8 hours with 6 3.06 GHz processors. The 7 ns production run took about 17 days with 12 2.4 GHz processors.

3.3 Results and discussion

3.3.1 Comparison between initial and final structures

The final structure after a 7 ns equilibration was minimized with conjugate gradient for 5,000 steps. The minimized mMrgC11/F-(D)M-R-F-NH₂ complex structure was superimposed with the initial structure by aligning TM C α atoms of the receptor. The RMSD for TM C α atoms was 2.50 Å. As expected, the loop regions were floppier (RMSD = 7.00 Å) and the most dramatic change was the closure of the binding site by the extracellular loop 2 (EC2). The formation of the 'lid' in the binding site by the EC2 was observed in bovine rhodopsin structure where the disulfide bond formed between two Cys residues in EC1 (closer to TM3) and EC2 stabilizes the

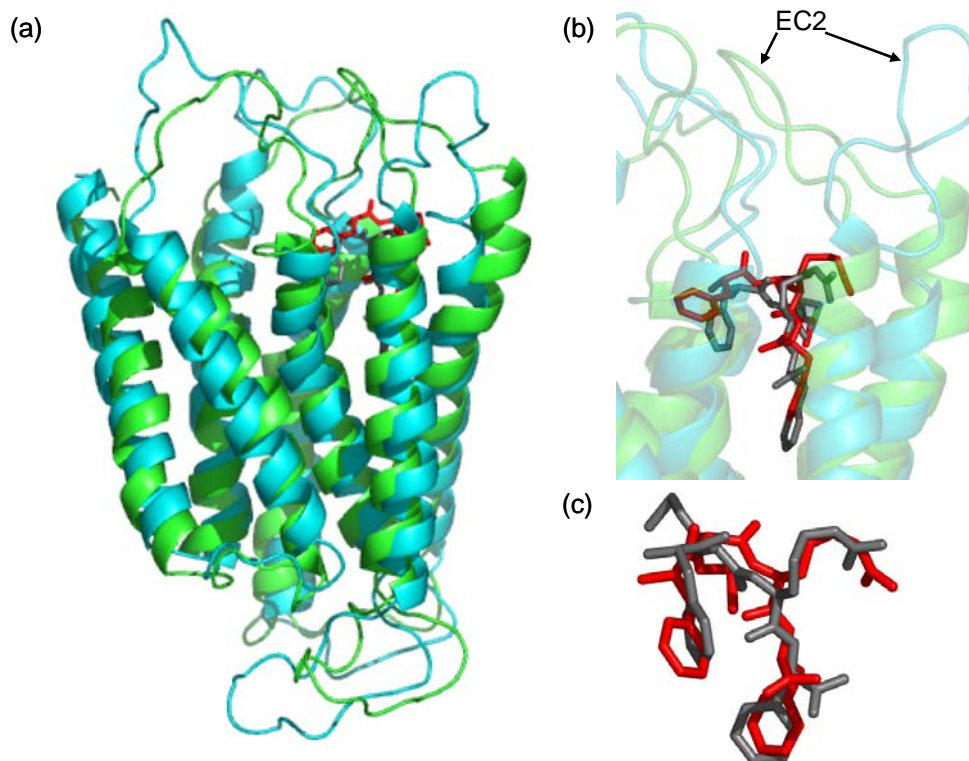


Figure 3.2 The mMrgC11/F-(D)M-R-F-NH₂ complex structure after 7 ns run. (a) Two complex structures at 0ns (cyan) and 7ns (green) are superimposed by aligning TM C α atoms between them. The ligands are colored in black for 0ns and in red for 7 ns. The water, lipid and ion molecules are removed for clarity. (b) The ligands are in close-up after the residues in 5 Å binding pocket are aligned (RMSD for ligand = 2.48 Å). (c) Two ligands at 0 and 7 ns are aligned with heavy atoms (RMSD = 1.83 Å).

closed conformation of the EC2[7]. These Cys residues are conserved in several GPCRs including amine receptors, and the presence of a ‘plug’ in the binding crevice was also suggested in the β 2 adrenergic receptor from the inaccessibility of quenchers to a fluorescent ligand[8]. The mMrgC11 receptor does not have the corresponding Cys residues and no disulfide bond is expected. However two oppositely charged residues, Lys96 (EC1) and Glu169 (EC2) are located at the similar sites and induce the closed conformation of EC2. If formation of a plug by EC2 is a general feature for all GPCRs, a key event in receptor activation would involve significant conformational change of EC2 allowing for rapid access of a ligand to the binding pocket.

The tetrapeptide ligand moved by $\sim 1.5 \text{ \AA}$ towards the extracellular regions after 7 ns equilibration, but not out of the binding pocket as shown in Figure 3.2(b). This kind of upward movement was also observed for the epinephrine agonist in the $\beta 2$ -adrenergic receptor after 4 ns of MD simulation in the presence of full membrane and water[9]. This behavior was distinct from rigidity shown in an antagonist case.

The conformation of F-(D)M-R-F-NH₂ was examined by aligning the heavy atoms of the ligand (Fig. 3.2(c)). Two Phe and Arg were relatively rigid since interactions with four aromatic residues (Tyr110, Phe190, Trp162 and Tyr256) and two Asp residues (Asp161 and Asp179) restrained their movement as predicted in chapter 2. The Met was labile and its side chain underwent a large conformation change, leading to 1.83 \AA of RMSD for the ligand.

3.3.2 Dynamic behavior in receptor conformation during MD simulation

The RMSD of C α atoms in the receptor was evaluated every 10 ps and plotted in Figure 3.3. Since the loop parts were much flexible, only the C α atoms in TM regions were used in alignment. The RMSD plot indicates that the TM regions became well equilibrated after 7 ns. To explore conformational fluctuation for each TM, the corresponding C α atoms were aligned respectively and then the RMSD of each TM was computed along the time. All TMs showed the similar plot (monotonous decrease) to Figure 3.3(a) of the whole TM regions. The large conformational change after 7 ns simulation was observed for TM6 and 7 (the RMSD values are 2.33 \AA and 2.36 \AA respectively). This conformational flexibility may be relevant to GPCR activation. The ligand binding is thought to trigger a cascade of structural changes in the receptor molecule that are capable of inducing activation of the associated G proteins. Here flexibility actually means low conformational barrier, leading to an ultimate structural change. The conformational change in TM6 of the rhodopsin or the $\beta 2$ adrenergic receptor was supported by several structural and photophysical experiments[10, 11]. Also the EPR study in rhodopsin

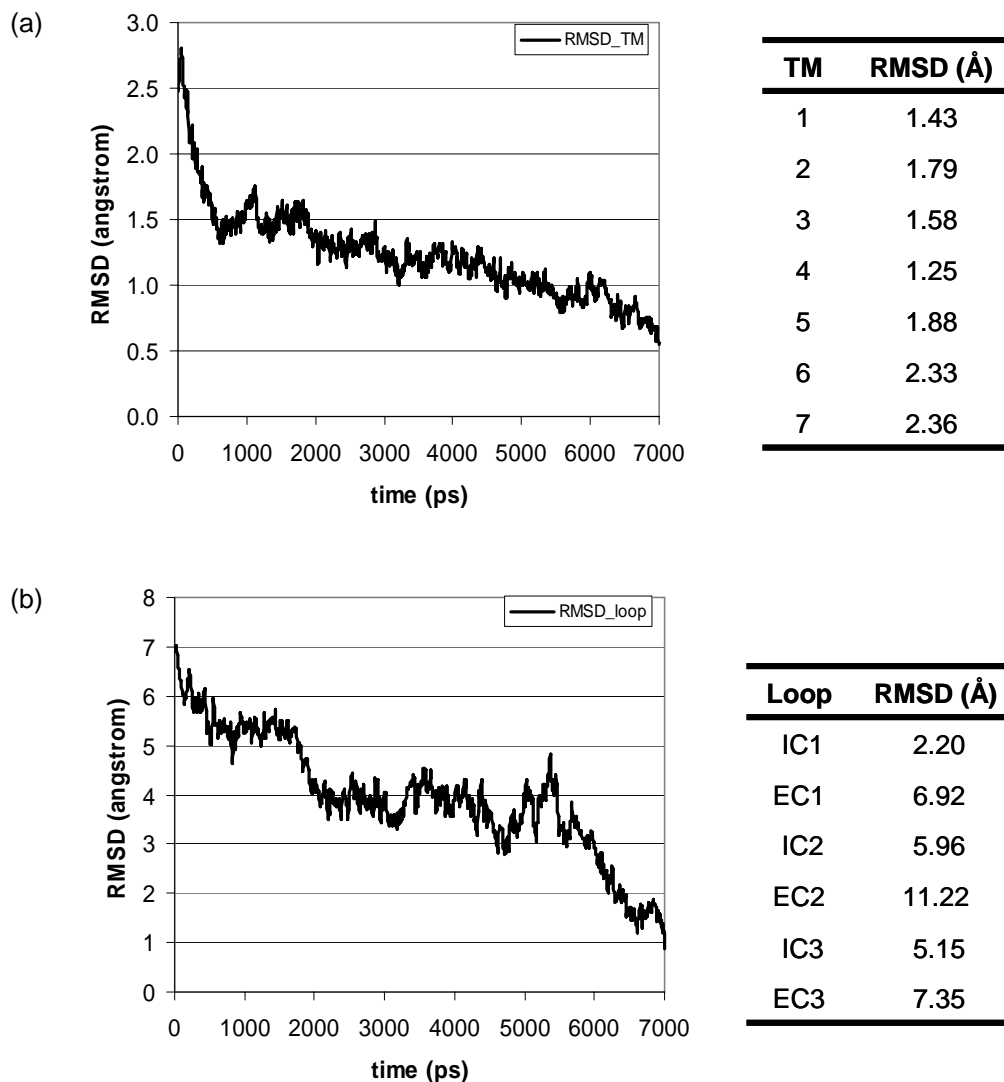


Figure 3.3 The RMSD fluctuation of $C\alpha$ atoms with respect to the final 7 ns structure. The RMSD is calculated every 10ps by aligning the $C\alpha$ atoms in TM regions. (a) The TM regions are selected. The RMSD values in table are calculated for the initial structure after aligning each TM respectively. (b) The whole loop part is selected in graph and each loop in table for RMSD calculation.

suggests that movement of the cytoplasmic end of TM7 relative to TM1 may occur in response of photoactivation[12].

The dramatic conformation change in loop regions was clearly demonstrated in the RMSD plot of Figure 3.3(b). Based on the RMSD value for each loop region (see table next to the RMSD plot), we can see that the extracellular loops underwent a larger conformational change. The most prominent change was for EC2 from an open to the closed conformation. The complete closure occurred after 6 ns and stayed until the end of simulation. Some conformational fluctuation was observed for EC1 and EC3 during the simulation. The dynamic behavior of the extracellular loop might be obvious since the ligand is bound in the upper half of TM regions from the extracellular region and directly perturbs the conformation of the residues close to the ligand.

Overall the significant change in the conformation of the receptor was seen in the mMrgC11/F-(D)M-R-F-NH₂ complex structure. Since F-(D)M-R-F-NH₂ is an agonist, the conformational change (from the inactive conformation to the active one) might be an apparent consequence.

3.3.3 Binding mode of F-(D)M-R-F-NH₂ after equilibration

The binding mode of the tetrapeptide F-(D)M-R-F-NH₂ after 7 ns equilibration is shown in Figure 3.4. The C-terminus amide group maintains the hydrogen bond with the side chain of Asp161 (TM4). The C-terminus F is still positioned in a stabilizing aromatic and hydrophobic environment formed by Tyr110 (TM3), Phe190 (TM5), Leu186 (TM5) and additionally Ile107 (TM3). The R is stabilized through the electrostatic interaction with Asp161 and an additional hydrogen bond with the side chain of Thr183 (TM5). However Asp179 in TM5 moved a little away from the R, but within the range where the electrostatic interaction was still effective (distance between NH1 of R and OD2 of Asp179 = 6.41 Å). The water molecules actually intervened in interaction between Asp179 and the ligand, and mediated a hydrogen bond between the side chain of Asp179 and the backbone carbonyl group of the ligand (Fig. 3.5). The

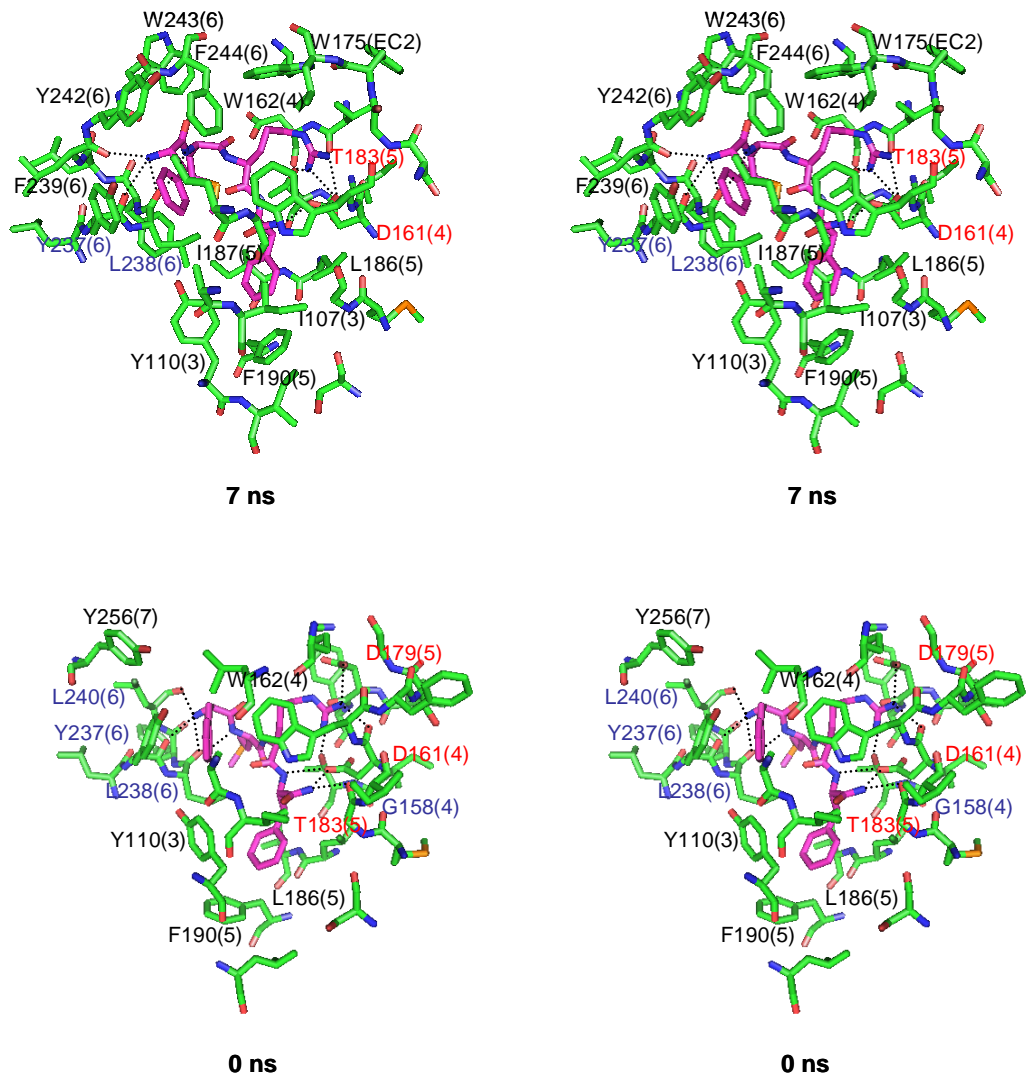


Figure 3.4 The 5 Å binding site of F-(D)M-R-F-NH₂ in mMrgC11 receptor. The intermolecular hydrogen bonds (calculated with explicit hydrogens using the same criteria as in Figure 2.4) are indicated by the dotted lines. A residue whose side chain participates in the hydrogen bond is specified in red, while one whose backbone is involved is in blue. The residues showing good hydrophobic interactions are specified in black. The top of each picture corresponds to the extracellular regions.

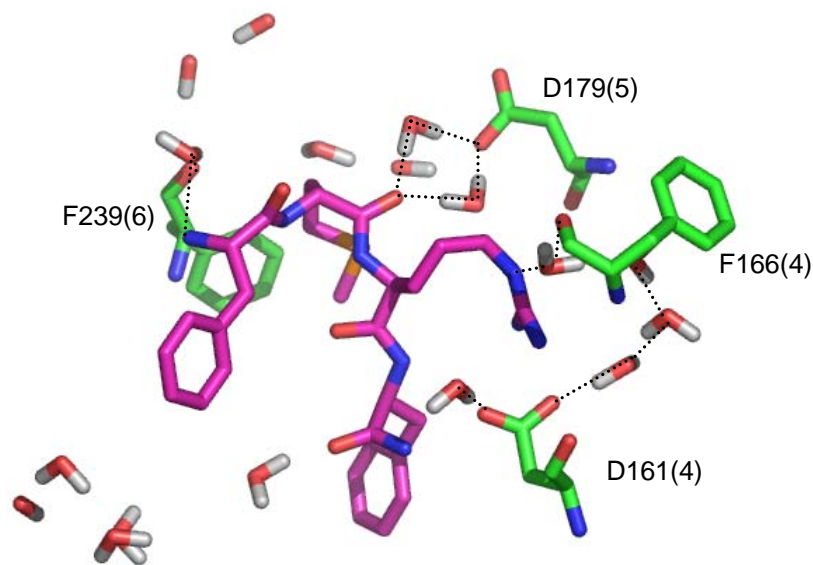


Figure 3.5 Water molecules in 5 Å binding pocket. The water-involved hydrogen bonds are indicated by the dotted line.

carboxylate group of Asp179 was solvated with more water molecules and also stabilized by the positively charged quaternary amine group of a lipid molecule (distance between N of quaternary amine and OD1 of Asp179 = 4.16 Å). This relatively weak interaction of Asp179 compared to Asp161 might be validated by our experimental observation in chapter 2. For the D161A mutant, four of the six agonists were rendered inactive, while the remaining two were only active at 100 times higher concentrations. Similarly, the D179A mutant showed no affinity for the three tetrapeptide agonists, while the other three were activated only at 10 times higher concentration of the ligand. This indicates that Asp161 should interact more effectively with the agonists than Asp179.

The N-terminal F remained sandwiched between Trp162 (TM4) and Tyr237 (TM6) (the closest C-C distances between two aromatic rings are 4.64 Å and 3.39 Å respectively). Two more aromatic residues in TM6, Tyr242 and Phe244 (located close to the extracellular loop) came into

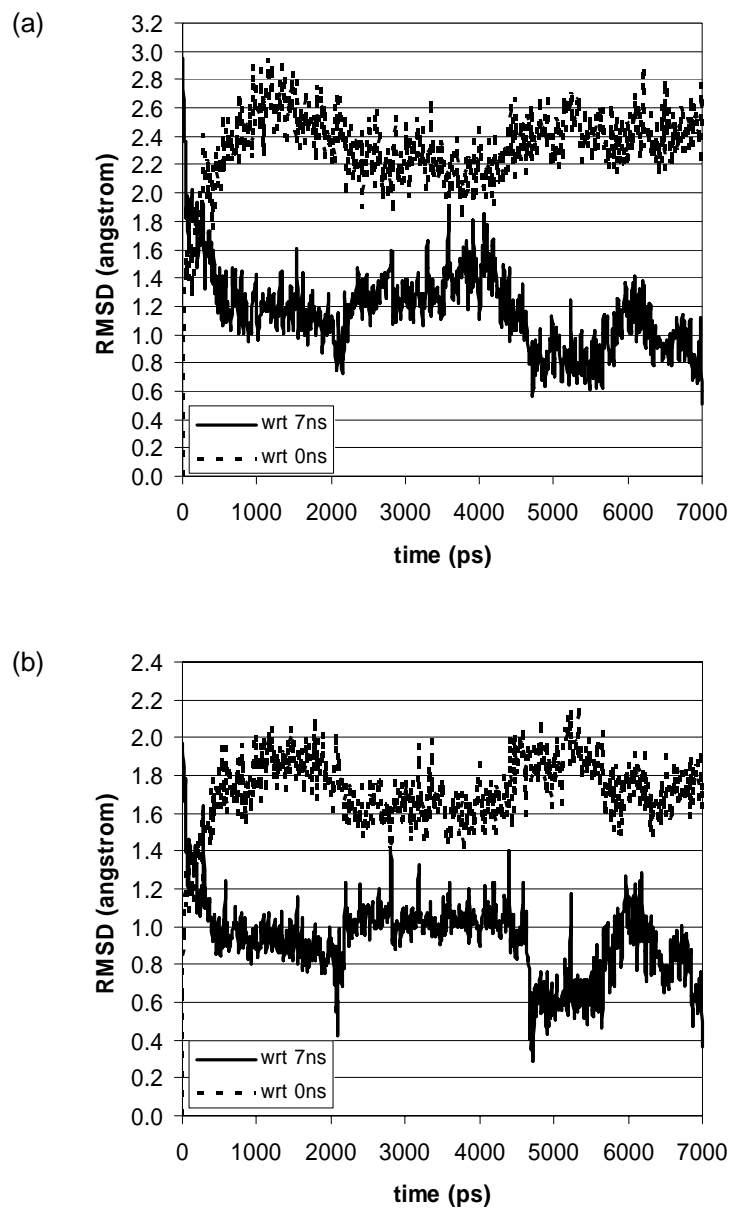


Figure 3.6 The RMSD fluctuation for ligand heavy atoms. (a) The residues in 5 Å binding pocket are aligned and then the RMSD for the ligand is computed. (b) The ligand parts are aligned each other. The real line is for the RMSD with respect to the final structure after a 7 ns equilibration and the dotted one for that with respect to the initial structure.

the binding pocket (the closest C-C distances between two aromatic rings are 4.22 Å and 3.40 Å respectively) and yielded the additional favorable aromatic interaction with the N-terminal F.

The water molecules filled the void in the binding pocket, forming hydrogen bonds with polar atoms, and some of them mediated an intermolecular hydrogen bond between the receptor and the ligand as observed for Asp179. The backbone atoms of Phe166 (TM4) and Phe239 (TM6) form the water-mediated hydrogen bonds with the side chain of R and the N-terminus of the tetrapeptide respectively.

3.3.4 Time profile of receptor-ligand interactions

Ligand conformation in the binding site

The RMSD of the ligand was evaluated every 10 ps in MD simulation. In Figure 3.6(a), the residues within the 5 Å binding pocket were used in alignment to give information about the ligand configurations in the binding site throughout time. The ligand was configurationally flexible and the RMSD of the final 7 ns minimized structure was 2.48 Å with the initial structure.

The ligand conformation itself fluctuated throughout the MD simulation and the RMSD values were ~1.5-2.0 Å with respect to the initial conformation. This indicates that the major contribution of configurational change shown previously is the conformational variation of the ligand itself. From the correlation between two RMSD plots (Fig. 3.6(a) and Fig. 3.6(b)) we can see that the ligand is confined within the binding pocket for 7ns, but exhibits conformational flexibility.

Intermolecular hydrogen bonds

The intermolecular hydrogen bonds between the receptor and the ligand were determined with the same criteria used in chapters 2 and 4 (see Fig. 4.3) for the initial and the final minimized structures. The distance between the donor and acceptor atoms was computed for every hydrogen bond pair and plotted along the time in Figure 3.7.

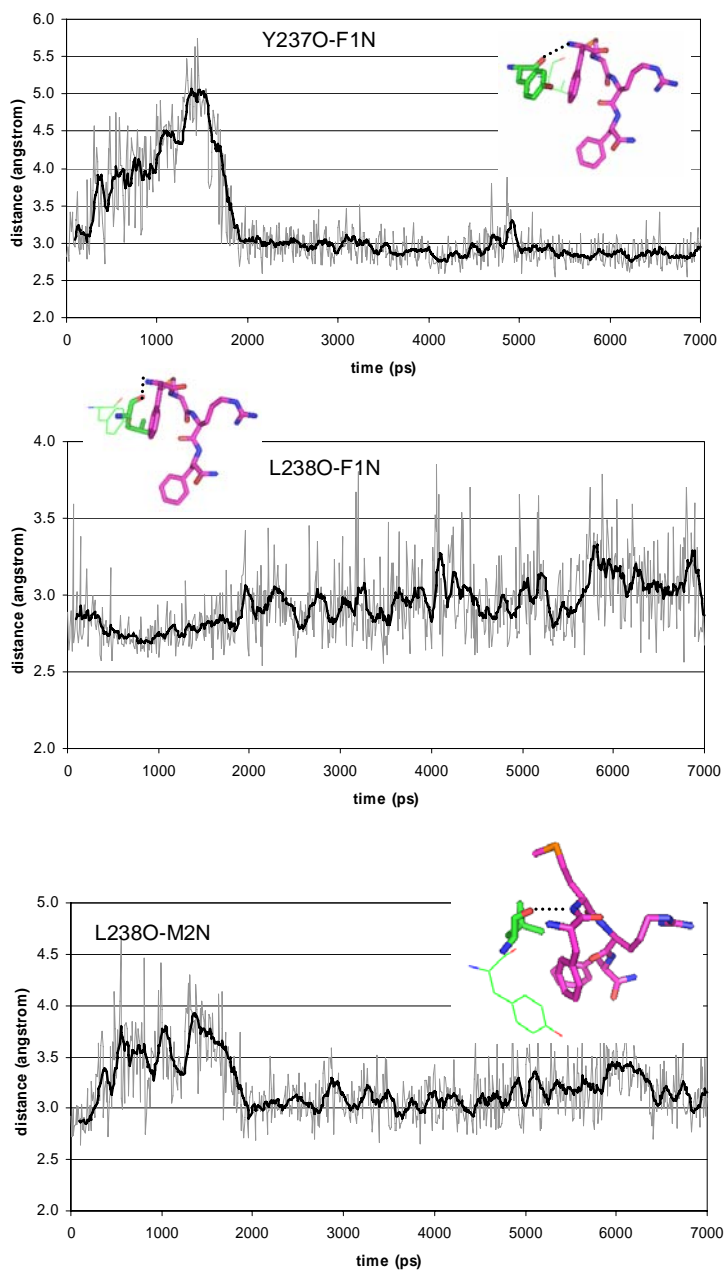


Figure 3.7 Time profile of intermolecular hydrogen bond distance. The distance is measured every 10 ps (grey). The moving average per 100 ps is in black. The hydrogen bond pair is indicated in this way: receptor part-ligand part with the index of [residue name][residue number][atom name participating in H-bond]. The ligand (carbon in purple) and the receptor residue (carbon in green) involved in the hydrogen bond is shown in stick at the picture. The corresponding hydrogen bond is indicated in the dotted line.

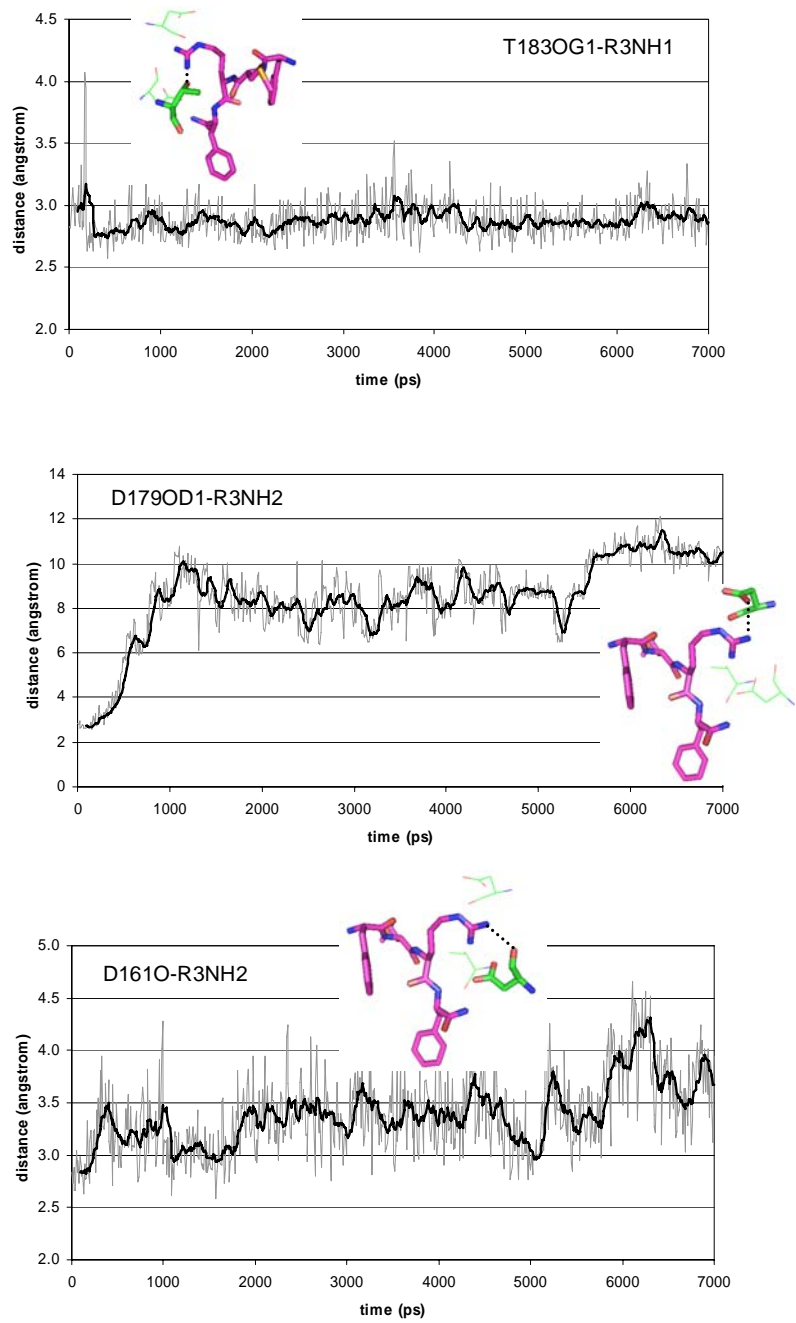


Figure 3.7 (continued)

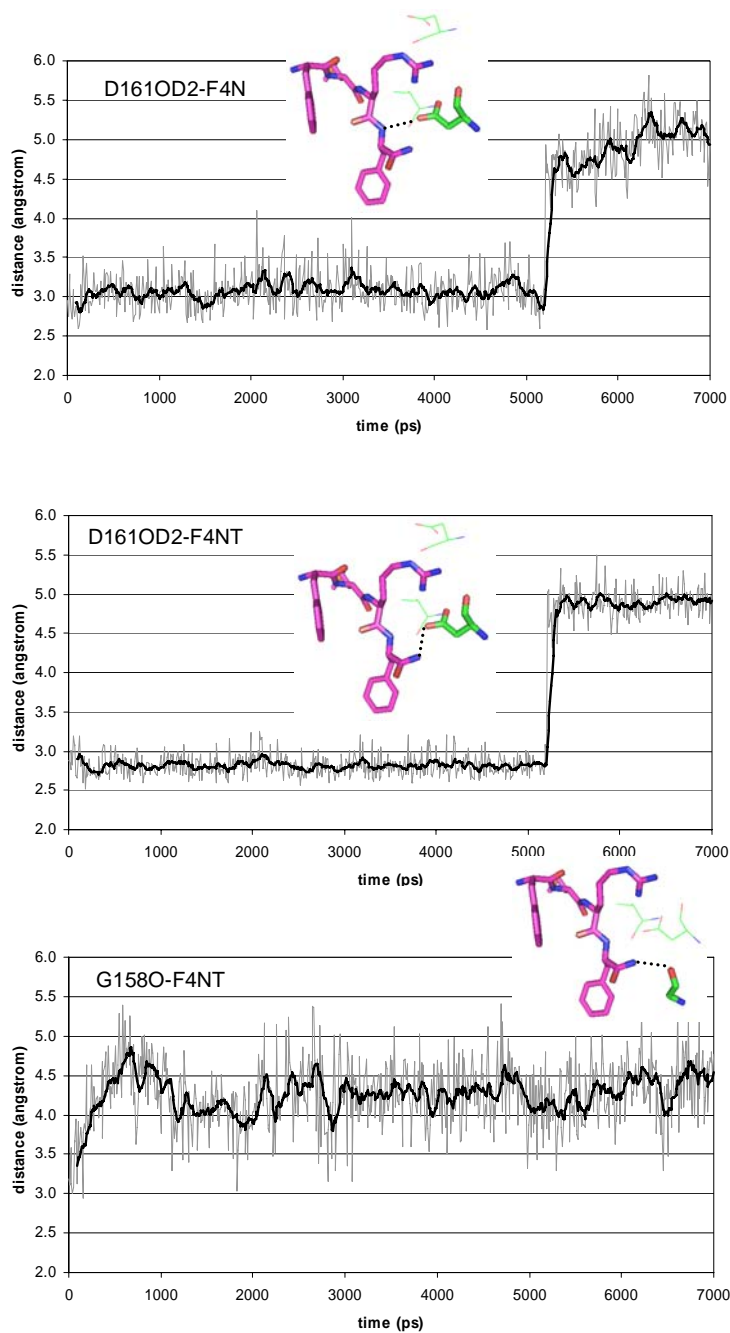


Figure 3.7 (continued)

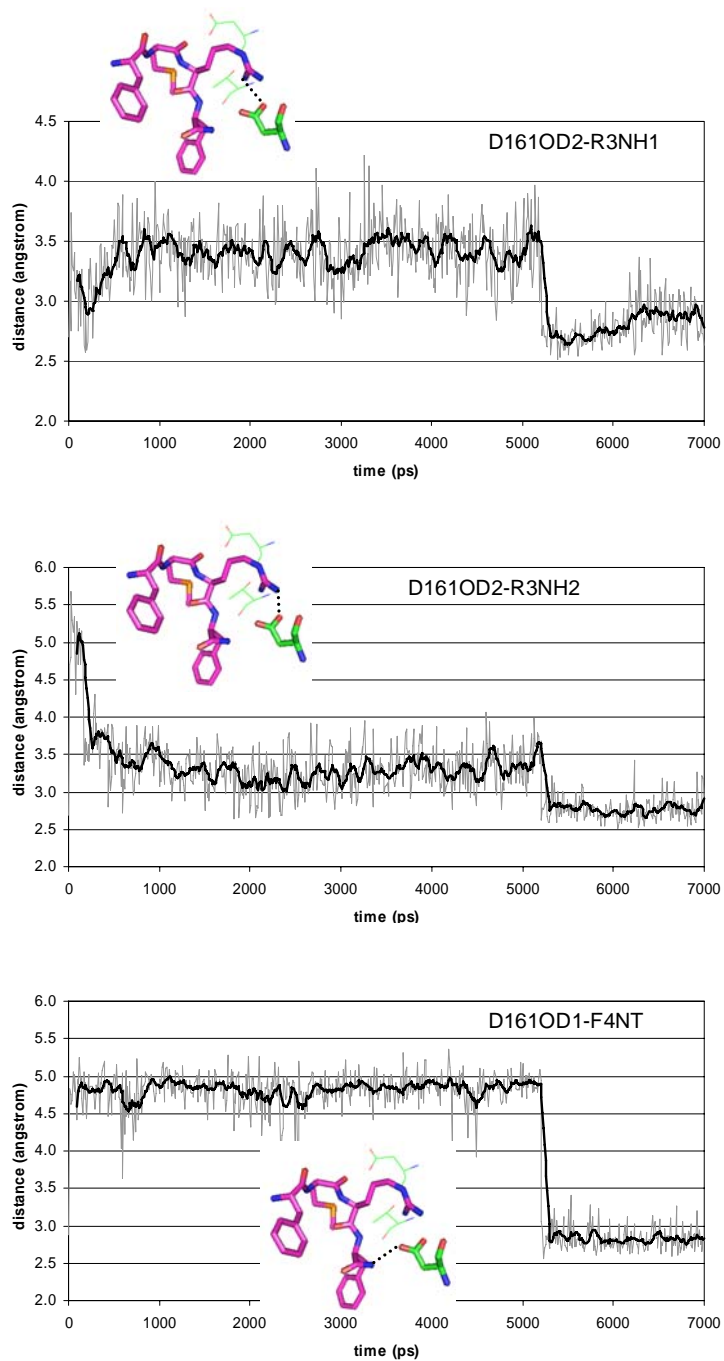


Figure 3.7 (continued)

The hydrogen bonds with the residues in TM6 (i.e. between the N-terminus and Tyr237 (Y237O-F1N) and between the backbone amide group and Leu238 (L238-M2N)) were interrupted for the first 2ns and then became stable. This observation indicates that some conformational rearrangement in (or near) TM6 occurs during these time frames. This fluctuation is well correlated with entry of Phe244 into the binding site as will be shown in Figure 3.8. The intrusion of Phe244 as well as Tyr242 perturbs the initial conformations, but the favorable interactions previously present are recovered after re-organization.

The direct hydrogen bond of the ligand with Asp179 became loose at the early stage due to a water molecule stepping in between them. However Asp179 still made contact with the ligand through the water-mediated hydrogen bond and electrostatic interaction. The side chain of R mostly interacted with the side chain of Asp161 in the ideal configuration after equilibration. The torsion χ_2 of the side chain in Asp161 was shown to be in relatively low barrier and the C-terminus amide group of the ligand switched a hydrogen bond partner between two carboxylate oxygen atoms of Asp161 after ~5 ns.

The hydrogen bond between the side chain of Thr183 and the side chain of R remained stable throughout the simulation period.

Inter-aromatic interaction

The time evolution of the centroid-to-centroid distance between two interacting aromatic rings was explored. The interaction of Tyr110 (TM3) and Phe190 (TM5) with the C-terminus F kept steady during 7 ns simulation. As mentioned previously, two more aromatic residues in TM6, Tyr242 and Phe244 participated in interaction with the N-terminal F after equilibration. Tyr242 came close at the early time step, but it did not interfere in the overall conformation of the binding site. However intrusion of Phe244 actually affected the present binding mode (note that Tyr237 and the N-terminal F become apart and back together) and then after conformational rearrangement all favorable aromatic interactions were recaptured.

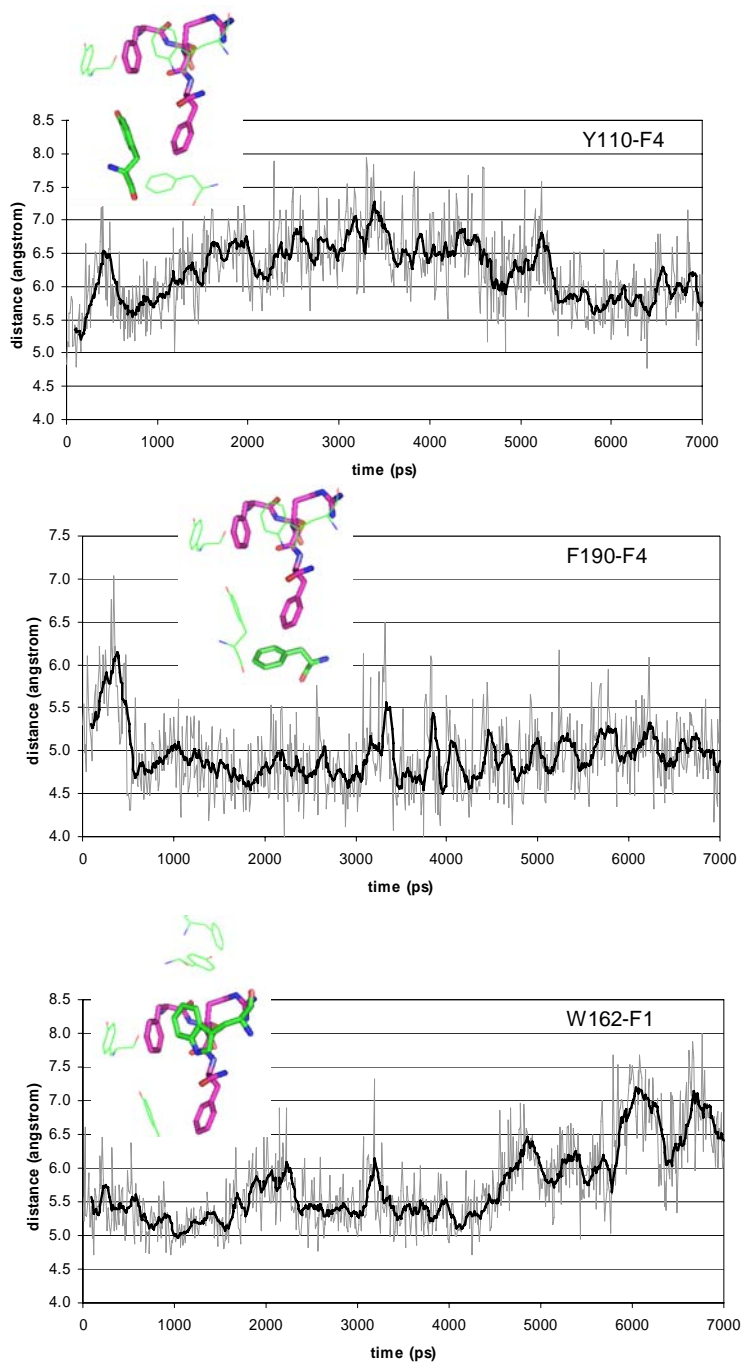


Figure 3.8 Time profile of centroid-to-centroid distance between two aromatic residues. F1 and F4 denote the N-terminal and C-terminal F of the tetrapeptide ligand respectively. The distance is measured every 10 ps (grey). The moving average per 100 ps is in black. The ligand (carbon in purple) and the receptor residue (carbon in green) are shown in stick at the picture. For tryptophan, the center of the six-membered ring is considered.

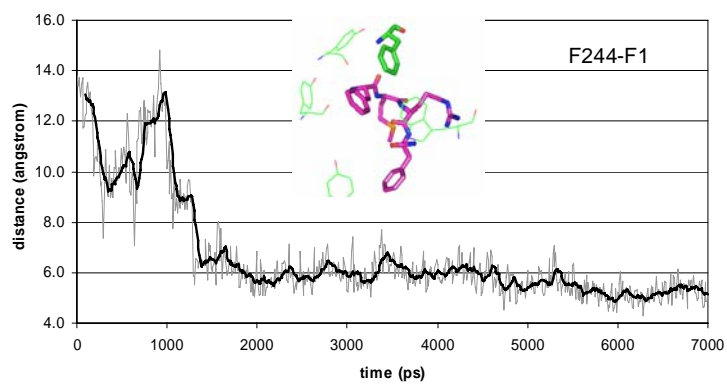
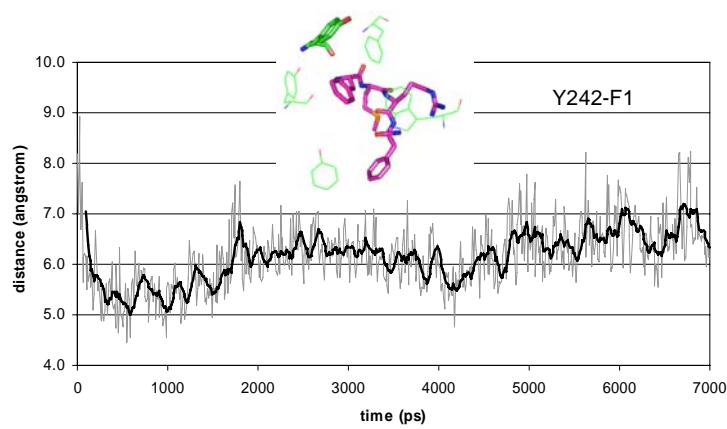
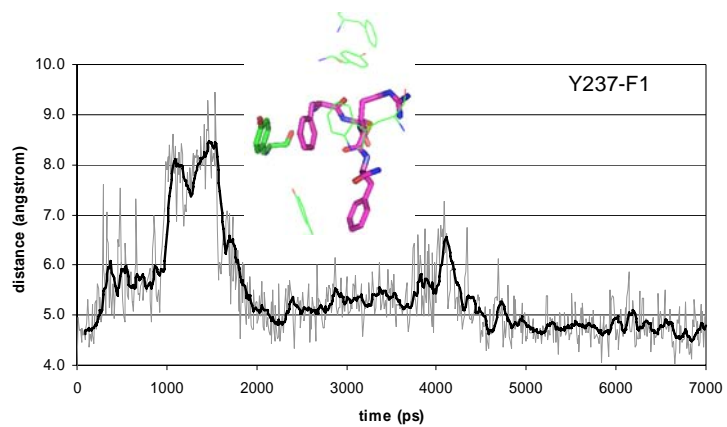


Figure 3.8 (continued)

The centroid distance at 7 ns showed that Trp162 (TM4) moved a little away from the ligand, and the closet C-C distance between aromatic rings of Trp162 and the N-terminal F was 4.64 Å. However Trp162 was not completely out of interaction with this F.

The stability of aromatic interactions identified in the previous prediction implies the accuracy of our predicted structure for the binding site. The new interactions with Tyr242 and Phe244 indicate that the explicit membrane and water simulation might be necessary to obtain correct conformations for residues on the boundary of the TM and the loop.

3.3.5 Time profile of inter-helical interactions

The nonbond distances between residues on different helices were analyzed to understand how the dynamics in the explicit lipid and water environment affect the inter-helical interactions. The inter-helical hydrogen bonds were identified for the initial and the final 7 ns minimized structure (Fig. 3.9) and the distances for these hydrogen bond pairs were measured throughout the MD simulation. The comparison of two hydrogen bond networks demonstrates some dynamic behavior on the inter-helical interactions. The initial hydrogen bond network was subjected to rearrangement during the MD simulation. We can also see some hydrogen bond pairs preserved after 7ns; Tyr63 (TM2) (one of the residues conserved in the Mrg receptor family (with 39 sequences available on Swiss-Prot and TrEMBL))–Ser112 (TM3) and Arg215 (TM6)–Val277 (TM7). Moreover the hydrogen bond between Tyr63 and Ser112 remained stable throughout the MD run as shown in Figure 3.10 and it may play a role in maintaining helix packing.

The hydrogen bond between Asn66 (TM4) and Trp151 (TM4) (the highly conserved residues in the family A of GPCRs that form an interhelical hydrogen bond in rhodopsin) became loose, but not totally apart. Asn66 partly formed a hydrogen bond with Ser115 (TM3) during the MD run.

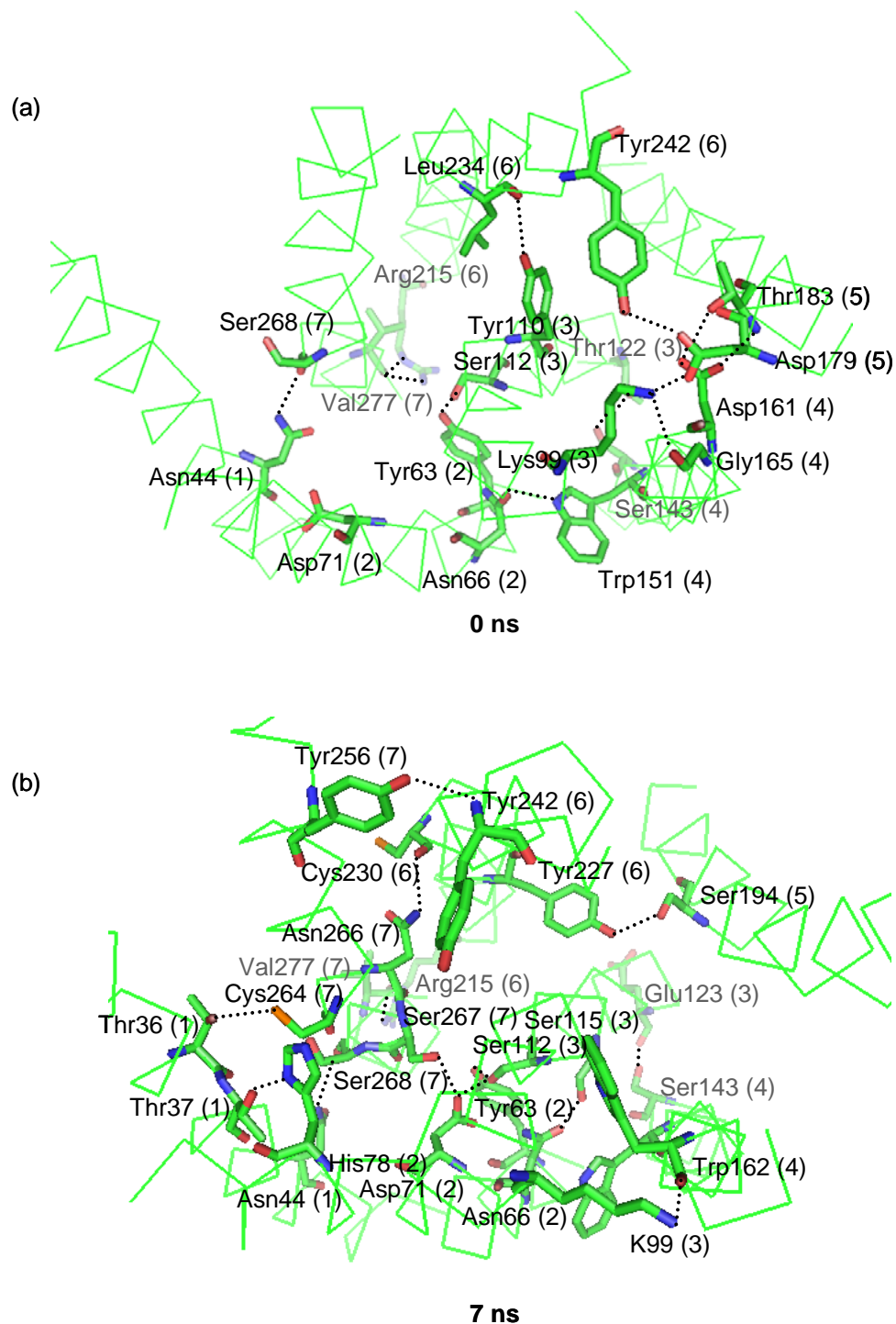


Figure 3.9 Interhelical hydrogen bond networks in the mMrgC11 receptor. It is viewed from the extracellular region. The interhelical hydrogen bonds (dashed lines) are specified with residues participating in hydrogen bond. (a) for the initial structure. (b) for the 7ns minimized structure. The HBPLUS program was used to calculate hydrogen bonds (maximum D-A distance = 3.9 Å, minimum D-H-A angle = 90.0°).

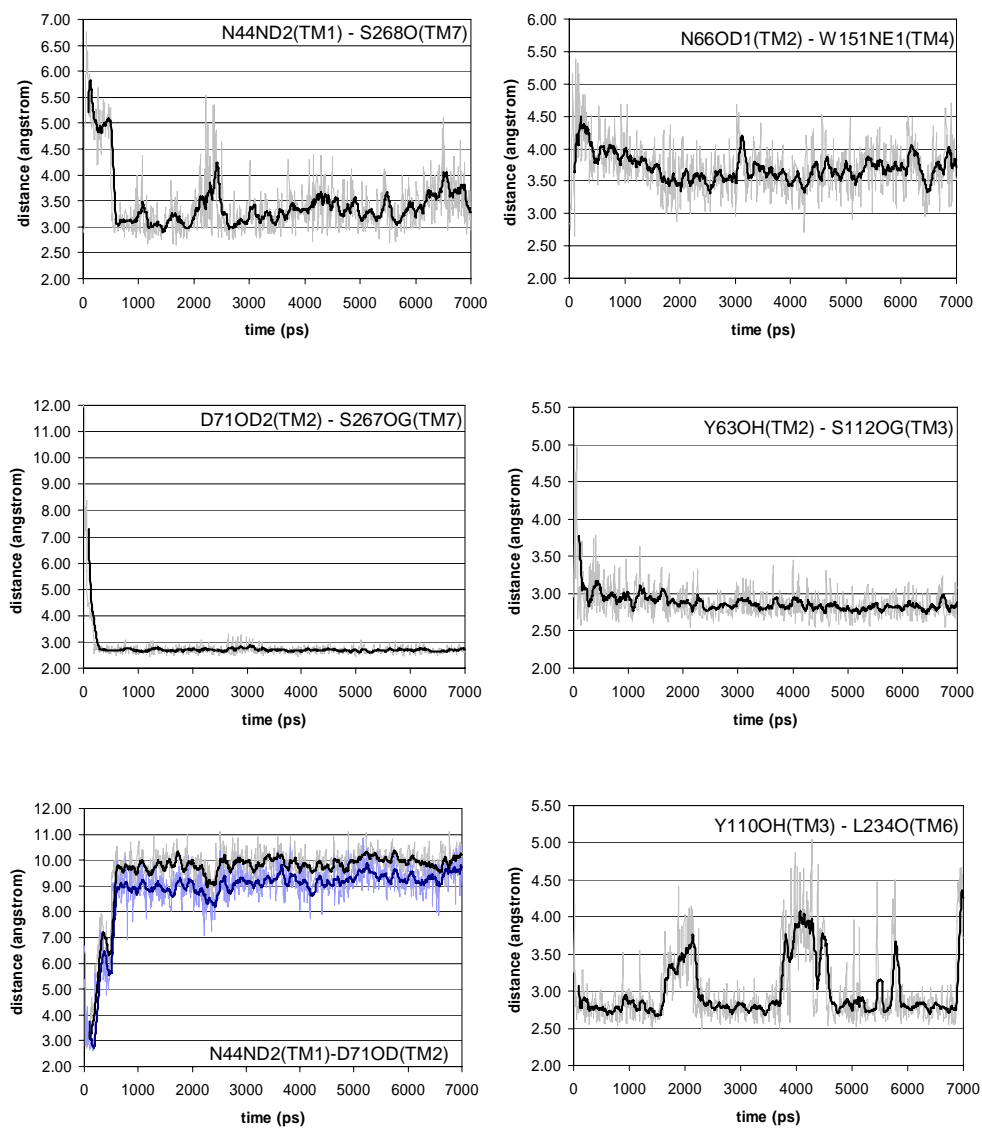


Figure 3.10 The time profile of the distance between residues residing in different helices. The same index rule ([residue name][residue number][atom name]) is used as in Figure 3.7.

Initially Asn44 (TM1) (highly conserved in the family A GPCRs) formed a hydrogen bond with the Ser268 carbonyl group of the backbone in TM7 as shown in Figure 3.9. This hydrogen bond was loosened for the early 500 ps (this may be an equilibration period needed for the protein structure to be adjusted from perturbation of the lipid and water molecules) and then the pair remained close enough for the hydrogen bond formation. At $t = 0$, Asp71 (TM2) that forms an inter-helical hydrogen bond with this Asn in rhodopsin was in the proximity, but was not in hydrogen bond contact in the mMrgC11 receptor. In the MD run the distance between Asp71 and Asn44 became larger, leading to ~ 9 -10 Å. Instead Asp71 moved close to TM7 and formed a stable hydrogen bond with Ser267. The approaching of TM2 and TM7 in the activated state was suggested for the angiotensin receptor II type 1 from mutation-induced constitutive activation, and later the *in situ* measurement of TM2 movement in the angiotensin receptor was also reported[13, 14]. Based on our simulation, it might be proposed that TM2 first moves further from TM1 on activation and then towards TM7. During 7ns, the concerted formation of hydrogen bonds in TM1, TM2 and TM7 that exists in the inactivated rhodopsin structure[7, 15] was not observed in our predicted mMrgC11 receptor, suggesting that the receptor structure was in the activated conformation.

Lastly we examined the distance between Tyr110 (TM3) and Leu234 (TM6). Tyr110 was one of the residues interacting with the ligand and underwent conformational fluctuation. This kind of flexibility between TM3 and TM6 may help induce the receptor activation.

3.4 Summary and conclusions

We performed the all-atom MD simulation of mMrgC11/F-(D)M-R-F-NH₂ structure in the explicit lipid and water environment. The analysis of the 7 ns MD trajectory clearly demonstrated that our predicted structure of the mMrgC11 receptor and its binding site of F-(D)M-R-F-NH₂ was stable in the full membrane system. The conformational flexibility of the side chain and small structural change in TM regions were present, but no significant instability was detected.

Moreover the initial interactions of the ligand with the key residues (Asp161 and four aromatic residues, Tyr110, Phe190, Trp162 and Tyr237) were preserved throughout the entire MD run except for Asp179 in TM5. Nevertheless Asp179 interacted with the ligand through water-mediated hydrogen bond and electrostatic interaction. These findings validate our structure prediction method, indicating that the MembStruk predicted structures are fairly accurate.

In addition we observed some dynamic behavior in protein structure. In the TM regions, TM6 and TM7 showed relatively large conformational change and it suggested the possibility of their implication in receptor activation. The loops underwent large structural fluctuations, and the most dramatic change was seen in EC2. Interestingly the electrostatic interaction of two oppositely charged residues, Glu169 (EC2) and Lys96 (EC1) pulled them each other, resulting in the closed conformation of EC2 that is similarly shown in rhodopsin. Two more aromatic residues in TM6, Tyr242 and Phe244 were newly identified to contact the N-terminal F of the ligand after the equilibration, securing the ligand in the binding site. They could be additional mutation candidates to be tested for the further validation. These observations indicate that the explicit membrane and water simulation might be necessary to obtain correct conformations for the loops, including residues on the boundary of the TM and the loop.

An extended simulation along with incorporation of G protein into our receptor structure where the intracellular loops are now fully equilibrated could be explored to examine the reciprocal effect of the G protein and the mMrgC11 receptor on the conformational change in activation. It would definitely provide the better understanding on the GPCR activation process.

References

1. Freddolino, P.L., et al., *Molecular dynamics simulations of the complete satellite tobacco mosaic virus*. *Structure*, 2006. **14**(3): p. 437-449.
2. Phillips, J.C., et al., *Scalable molecular dynamics with NAMD*. *Journal of Computational Chemistry*, 2005. **26**(16): p. 1781-1802.
3. Hall, S.E., *Development of a structure prediction method for G-protein coupled receptors*, in *Division of Chemistry and Chemical Engineering*. 2005, California Institute of Technology: Pasadena.
4. Mackerell, A.D., et al., *Self-Consistent Parameterization of Biomolecules for Molecular Modeling and Condensed Phase Simulations*. *Faseb Journal*, 1992. **6**(1): p. A143-A143.
5. MacKerell, A.D., et al., *All-atom empirical potential for molecular modeling and dynamics studies of proteins*. *Journal of Physical Chemistry B*, 1998. **102**(18): p. 3586-3616.
6. Jorgensen, W.L., et al., *Comparison of Simple Potential Functions for Simulating Liquid Water*. *Journal of Chemical Physics*, 1983. **79**(2): p. 926-935.
7. Okada, T., et al., *The retinal conformation and its environment in rhodopsin in light of a new 2.2 angstrom crystal structure*. *Journal of Molecular Biology*, 2004. **342**(2): p. 571-583.
8. Tota, M.R. and C.D. Strader, *Characterization of the Binding Domain of the Beta-Adrenergic-Receptor with the Fluorescent Antagonist Carazolol - Evidence for a Buried Ligand-Binding Site*. *Journal of Biological Chemistry*, 1990. **265**(28): p. 16891-16897.
9. Spijker, P., et al., *Dynamic behavior of fully solvated beta 2-adrenergic receptor, embedded in the membrane with bound agonist or antagonist*. *Proceedings of the*

- National Academy of Sciences of the United States of America, 2006. **103**(13): p. 4882-4887.
10. Farrens, D.L., et al., *Requirement of rigid-body motion of transmembrane helices for light activation of rhodopsin*. *Science*, 1996. **274**(5288): p. 768-770.
 11. Ghanouni, P., et al., *Agonist-induced conformational changes in the G-protein-coupling domain of the beta(2) adrenergic receptor*. *Proceedings of the National Academy of Sciences of the United States of America*, 2001. **98**(11): p. 5997-6002.
 12. Altenbach, C., et al., *Structure and function in rhodopsin: Mapping light-dependent changes in distance between residue 65 in helix TM1 and residues in the sequence 306-319 at the cytoplasmic end of helix TM7 and in helix H8*. *Biochemistry*, 2001. **40**(51): p. 15483-15492.
 13. Groblewski, T., et al., *Mutation of Asn(111) in the third transmembrane domain of the AT(1A) angiotensin II receptor induces its constitutive activation*. *Journal of Biological Chemistry*, 1997. **272**(3): p. 1822-1826.
 14. Miura, S. and S.S. Karnik, *Constitutive activation of angiotensin II type I receptor alters the orientation of transmembrane helix-2*. *Journal of Biological Chemistry*, 2002. **277**(27): p. 24299-24305.
 15. Palczewski, K., et al., *Crystal structure of rhodopsin: A G protein-coupled receptor*. *Science*, 2000. **289**(5480): p. 739-745.